

Sprouty4 correlates with favorable prognosis in perihilar cholangiocarcinoma by blocking the FGFR-ERK signaling pathway and arresting the cell cycle

Bo Qiu^{a,1}, Tianli Chen^{a,1}, Rongqi Sun^a, Zengli Liu^a, Xiaoming Zhang^b, Zhipeng Li^c, Yunfei Xu^{a,*}, Zongli Zhang^{a,*}

^a Department of General Surgery, Qilu Hospital of Shandong University, 107 Wenhua Road, Jinan, Shandong, China

^b Department of General Surgery, Linyi People's Hospital, Linyi, China

^c Department of General Surgery, Shandong Provincial Hospital, Jinan, China

ARTICLE INFO

Article History:

Received 3 September 2019

Revised 9 November 2019

Accepted 12 November 2019

Available online 22 November 2019

Keywords:

Sprouty 4

Perihilar cholangiocarcinoma

Prognosis

Proliferation

Cell cycle

ABSTRACT

Background: Perihilar cholangiocarcinoma (PHCC) is the most common subtype of cholangiocarcinoma (CCA). We previously investigated the expression pattern of Sprouty (SPRY) in intrahepatic cholangiocarcinoma (ICC), but the expression and clinical significance of SPRY family members in PHCC are still unknown.

Methods: The expression of SPRY family members (SPRY1–4) was detected in different subtypes of CCA and corresponding adjacent tissues. SPRY4 expression in 142 cases of PHCC was detected by immunohistochemistry, and its clinical significance was evaluated using univariate and multivariate analyses. The functions of SPRY4 in the FGFR-induced proliferation and migration of PHCC cells were investigated through *in vitro* and *in vivo* experiments. We further investigated the effects and mechanisms of SPRY4 on FGFR-induced ERK phosphorylation and cell cycle distribution in the presence of FGFR and ERK inhibitors.

Findings: SPRY4 was the only SPRY family member associated with PHCC prognosis, and it was identified as an independent factor predicting favorable prognosis. In PHCC, SPRY4 expression was extensively associated with FGFR2, and its expression can be induced by ectopic FGFR2 activation. Through *in vitro* and *in vivo* experiments, we demonstrated that SPRY4 suppressed FGFR-induced proliferation and migration by inhibiting ERK phosphorylation. Moreover, SPRY4 knockdown was shown to decrease the percentage of cells in the G1 phase and promote the percentage of cells in the S and G2/M phases by increasing cyclin D1 expression, which also required FGFR-induced ERK phosphorylation.

Interpretation: High expression of SPRY4 was an independent biomarker of favorable prognosis in PHCC. SPRY4 expression can be induced by ectopic FGFR2 activation in PHCC. SPRY4 arrested the cell cycle at G1 phase and suppressed FGFR-induced proliferation and migration by inhibiting ERK phosphorylation, indicating that SPRY4 may be a potential therapeutic target in PHCC.

© 2019 The Authors. Published by Elsevier B.V. This is an open access article under the CC BY-NC-ND license. (<http://creativecommons.org/licenses/by-nc-nd/4.0/>)

Abbreviations: CCA, cholangiocarcinoma; PHCC, perihilar cholangiocarcinoma; ICC, intrahepatic cholangiocarcinoma; DCC, distal cholangiocarcinoma; AJCC/UICC, American Joint Committee on Cancer/Union for International Cancer Control; SPRY, sprouty; IDH, isocitrate dehydrogenase; TMA, tissue microarray; OS, overall survival; FBS, fetal bovine serum; PBS, phosphate-buffered saline; IHC, immunohistochemistry; SDS-PAGE, sodium dodecyl sulfate polyacrylamide gel electrophoresis; PVDF, polyvinylidene fluoride; qRT-PCR, quantitative real-time PCR; CCK-8, cell counting kit-8; FACS, fluorescence-activated cell sorting; KRAS, Kirsten rat sarcoma viral oncogene; MAPK, mitogen-activated protein kinase; ERK, extracellular regulated protein kinase; FGFR, fibroblast growth factor receptor; EGFR, epidermal growth factor receptor.

* Corresponding authors.

E-mail addresses: xuyunfei1988@126.com (Y. Xu), zzlzl1900@163.com (Z. Zhang).

¹ These authors contributed equally.

1. Introduction

Cholangiocarcinoma (CCA) is a type of malignancy arising from the biliary tree. Patients with CCA usually suffer from late diagnosis and poor outcomes [1]. The incidence of CCA is increasing worldwide, especially in East and Southeast Asia [2]. Based on the anatomical location of the tumor, CCA can be further classified into subtypes including intrahepatic (ICC), perihilar (PHCC), and distal (DCC) cholangiocarcinoma, with distinct risk factors, molecular pathogenesis, biological features, clinical characteristics and treatment strategies. PHCC is the most common type of CCA, accounting for more than 50% of cases [3]. Radical surgery is a curative option for all CCA subtypes but is extremely difficult for PHCC because of the anatomical

Research in context

Evidence before this study

Perihilar cholangiocarcinoma (PHCC) is the most common subtype of cholangiocarcinoma (CCA) with the worst prognosis. Studies of new biomarkers or molecular profiles for PHCC have remained stagnant compared with those for intrahepatic cholangiocarcinoma (ICC), because radical resection of PHCC is much more difficult to achieve. The poor prognosis of PHCC is partially because of the lack of effective adjuvant therapy. The effects of chemotherapy or radiotherapy are limited, and there is no FDA-approved targeted drug for PHCC.

Added value of this study

In our study, for the first time, we compared the expression all SPRY family members in different subtypes of CCA and investigated their prognostic significance in PHCC. Consequently, we demonstrated that SPRY4 was notably associated with tumor size and lymphatic invasion and that it was an independent prognostic biomarker in PHCC. Through *in vitro* and *in vivo* experiments, we demonstrated that SPRY4 could suppress FGFR-induced proliferation and migration of PHCC by inhibiting ERK phosphorylation. Furthermore, we revealed that SPRY4 inhibited proliferation by arresting cells in the G1 phase via a reduction in cyclin D1 expression.

Implications of all the available evidence

Our results indicated that SPRY4 may be a potential therapeutic target in PHCC and that drugs activating SPRY4 may be promising for treating PHCC because the relevant preclinical drugs are antagonists. Regarding clinical application, our results suggested that the detection of SPRY4 in PHCC patients may help stratify high- and low-risk patients more effectively, which may guide individualized therapy in PHCC.

complexity of the perihilar region [4]. The prognosis of PHCC is still very dismal (<30% in most studies), although surgical techniques and adjuvant therapy have been dramatically improved [5].

Technological revolution, such as second-generation sequencing, provides more insights into the molecular characteristics and therapeutic strategies for tumor treatment. This is especially important to biliary cancer, including CCA, because more than 65% of patients with biliary cancer are diagnosed with unresectable disease [6]. Emerging evidence from comprehensive genetic analyses reveal several actionable mutations in CCA, such as fibroblast growth factor receptor (FGFR) fusion rearrangements and isocitrate dehydrogenase (IDH)-1 and IDH2 mutations. However, studies on the molecular patterns and features of PHCC are lagging behind those for ICC, despite PHCC having the highest prevalence. No study has regarded PHCC as a distinct cancer type in comprehensive genetic analysis thus far, although PHCC and DCC have been identified as different extrahepatic CCA since 2007 by the 7th American Joint Committee on Cancer/Union for International Cancer Control (AJCC/UICC) system.

In all subtypes of CCA, Kirsten ras sarcoma viral oncogene homolog (KRAS) mutations and FGFR2 fusions are well-identified somatic genetic alterations [7]. KRAS mutations are associated with poor overall survival [8], and several independent lines of evidence have demonstrated the role of FGFR2 fusion in CCA tumorigenesis and progression [9–11]. FGFR2 is a receptor tyrosine kinase involved in cellular processes such as proliferation mainly by activating downstream pathways, including Ras/Raf/MEK/MAPK and PI3K/AKT signaling [12]. RAS is a member of the FGFR2 signaling pathway, and its

common downstream signaling pathway is the MEK/MAPK pathway. Both KRAS mutations and FGFR2 fusions constitutively stimulate the MEK/MAPK pathway, and this ectopic activation finally leads to excessive proliferation in tumor cells. ERK, one of the most famous MAPKs, is a main effector downstream of both KRAS and FGFR2.

It is well accepted that RAS activation can initiate compensatory feedback mechanisms that attenuate signaling output [13]. The sprouty (SPRY) family, comprising SPRY1–4, is the most important negative regulator of the Ras/Raf/MEK/MAPK signaling pathway [14]. SPRY can inhibit ERK phosphorylation by modulating the FGFR/Ras/Raf/MEK/MAPK pathway at different levels [15,16]. Dysfunction in the SPRY family has been reported to be correlated with progression in several types of cancers, including gastric cancer, breast cancer, liver cancer and prostate cancer [17–24]. However, emerging evidence indicates that the expression of SPRY members is tumor-specific and that not all SPRY members are involved in the progression and prognosis of different cancer types. For example, SPRY4 was reported to inhibit the tumorigenesis in several tumor types like lung cancer and glioblastoma [25,26].

SPRY2, but not SPRY4, is an independent prognostic biomarker for human epithelial ovarian cancer [27]. Moreover, loss of SPRY4 but not of other SPRY members, amplifies RAS signaling in acute myeloid leukemia [28]. In our previous study, we demonstrated that different SPRY members had different expression patterns in ICC and that SPRY2 suppressed the progression of ICC by antagonizing FGFR2 signaling [29]. Nevertheless, the expression, function and clinical significance of the SPRY family in PHCC are still unknown.

In our study, we investigated the expression of SPRY family members in ICC, PHCC and DCC to identify the key effector responsible for Ras/Raf/MEK/MAPK signal feedback in PHCC cells and evaluated its clinical significance by analyzing the correlations between clinicopathological factors and survival time. Through *in vitro* and *in vivo* experiments, we further evaluated the oncogenic function of SPRY4 in PHCC progression and explore the underlying mechanism of SPRY4-suppressed progression of PHCC.

2. Materials and methods

2.1. Patients and follow-up

The primary cohort of our study comprised 424 patients who underwent surgery for PHCC at Qilu Hospital of Shandong University from 2007 to 2018. A validation cohort consisting of 142 patients was further selected according to the following inclusion criteria: (i) patients who underwent radical resection with a clear surgical margin; (ii) patients with available formalin-fixed tumor tissues, follow-up information and complete medical records; (iii) patients with postsurgical survival time of more than 1 month; and (iv) patients with no history of other malignancies. Tumor tissues and adjacent tissues of ICC, PHCC and DCC were collected during surgical resection on the premise of not interfering with the pathological diagnosis. The tumors were classified and staged according to the 8th AJCC/UICC TNM classification system. Informed consent was obtained from all patients. All experiments were approved by the Ethical Committee of Qilu Hospital of Shandong University.

2.2. Tissue microarray construction, immunohistochemistry and scoring

Tissue microarrays (TMAs) of formalin-fixed and paraffin-embedded tissue sections were made according to a previous report [30]. A senior pathologist was responsible for selecting representative tumor areas for TMAs by staining sections with hematoxylin and eosin. The expression of SPRY4 in PHCC was investigated with immunohistochemistry (IHC) described in detail in a previous study [29]. Stained TMAs were screened by a TMA scanner (Panoramic MIDI, 3D HISTECH, Budapest, Hungary), and the results of IHC were quantified

with histochemistry scores (H-scores), which were generated by Quant Center software and defined as H-score = (percentage of cells with weak staining intensity \times 1) + (percentage of cells with moderate staining intensity \times 2) + (percentage of cells with strong staining intensity \times 3) according to previous studies [31, 32]. The cohort was divided into subgroups according to the cut-offs of H-scores, which were identified as the point with the highest sum of specificity and sensitivity in the receiver operating characteristic (ROC) curve according to a previous study [33].

2.3. Cells and agents

Human ICC cell lines RBE and HCCC-9810 and PHCC cell lines FRH0201 and QBC939 were purchased from Cell Bank of the Chinese Academy of Sciences (Shanghai, China) or American Type Culture Collection (Manassas, VA, USA). RBE, FRH0201, and HCCC-9810 were maintained in RPMI-1640 medium (Gibco, Grand Island, New York, USA), and QBC939 was maintained in DMEM (Gibco), containing 10% fetal bovine serum (FBS; Gibco), and 100 U/ml penicillin and streptomycin (Gibco).

Primary antibodies were as follows: anti-SPRY1 (Abcam, Cambridge, UK; Cat. No. ab111523), anti-SPRY2 (Santa Cruz, CA, USA; Cat. No. sc-100862), anti-SPRY3 (Abcam, Cat.No. ab233424), anti-SPRY4 (Santa Cruz, Cat.No. sc-18609), anti-ERK1/2 (Cell Signaling Technology, Cat.No. 4695T), anti-phospho-ERK1/2 (Cell Signaling Technology, Cat.No. 4370T), anti-Bax (Abcam, Cat.No. ab32503), anti-Bcl-2 (Abcam, Cat.No. ab32124), anti-caspase-3 (Abcam, Cat.No. ab32351), anti-Cyclin A2 (Abcam, Cat.No. ab181591), anti-Cyclin B1 (Cell Signaling Technology, Cat.No. 12231), and anti-Cyclin D1 (Cell Signaling Technology, Cat.No. 2978).

2.4. RNA extraction and RT-PCR

Total mRNA was isolated from cultured cells, CCA tissues and adjacent normal tissues by using TRIzol reagent (Invitrogen, California, USA). Reverse transcription was performed using the ReverTra Ace qPCR RT kit (TOYOBO, Japan). Quantitative real-time PCR (qRT-PCR) was carried out using SYBR Green Master Mix (Roche, USA), and GAPDH RNA was used as an internal control. Relative mRNA levels were analyzed by the $2^{-\Delta\Delta CT}$ and $2^{-\Delta CT}$ methods. The primers were as follows:

SPRY1 forward: 5'-TCCTGTTTGGCCTGTAACCG-3'
 SPRY1 reverse: 5'-TCGTCGTCATTTGGAGCAGTG-3'
 SPRY2 forward: 5'-CCCTCTGTCCAGATCCATA-3'
 SPRY2 reverse: 5'-CCCAAATCTTCTTGCTCAG-3'
 SPRY3 forward: 5'-TTGCCAGCTCAATGTCCTCAT-3'
 SPRY3 reverse: 5'-CGGATGATGGATTGGCCTGA-3'
 SPRY4 forward: 5'-TCTGACCAACGGCTTTAGAC-3'
 SPRY4 reverse: 5'-GTGCCATAGTTGACCAGAGTC-3'
 Cyclin A2 forward: 5'-GGTACTGAAGTCCGGGAACC-3'
 Cyclin A2 reverse: 5'-TGCTTTCCAAGGAGGAACGG-3'
 Cyclin B1 forward: 5'-GCACTTCTTCGGAGAGCAT-3'
 Cyclin B1 reverse: 5'-GTTCTTGACAGTCCATTACCA-3'
 Cyclin D1 forward: 5'-GATGCCAACCTCTCAACGA-3'
 Cyclin D1 reverse: 5'-GGAAGCGGTCCAGGTAGTTC-3'
 GAPDH forward: 5'-GAGTCAACGGATTTGGTCGT-3'
 GAPDH reverse: 5'-GACAAGCTTCCCGTTCTCAG-3'

2.5. Cell transfection and establishment of stable cell lines

QBC939 cells were seeded in 6-well plates (3×10^5 /well) and incubated for 24 h. An shRNA targeting SPRY4 was transfected into cells via lentiviruses (GenePharma, Shanghai, China) with 5 μ g/ml polybrene (GenePharma). The cells were incubated in complete medium containing 4 μ g/ml puromycin for 10 days to obtain stable cell lines. A scramble sequence was used as a negative control. The

efficiency of knockdown was verified by western blotting analysis and qRT-PCR. The sequences of shRNA were as follows: scrambled sense sequences: 5'-UUCUCCGAACGUGUCACGUTT-3' scrambled anti-sense sequence: 5'-ACGUGACACGUUCCGAGAATT-3'

SPRY4 sense sequences: 5'-GCCUGUUUCUCCGUACAGUTT-3'

SPRY4 anti-sense sequence: 5'-ACUGUACGGAGAAACAGGCTT-3'

2.6. Western blotting analysis

Cells and tissues were lysed using RIPA (Beyotime, Shanghai, China) with 1% phenylmethylsulfonyl fluoride (PMSF; Beyotime) and 1% phosphatase inhibitor (Solarbio, Beijing, China)[34]. Total proteins were separated by 10% sodium dodecyl sulfate polyacrylamide gel electrophoresis (SDS-PAGE) and transferred to polyvinylidene fluoride (PVDF) membranes. The membranes were incubated with primary antibodies overnight and then incubated with secondary antibodies for 1.5 h. Proteins were finally visualized using enhanced chemiluminescence (Millipore, Bedford, MA, USA). The results of western blotting were quantified by ImageJ software if necessary.

2.7. Wound healing assay

Cells were seeded into 6-well plates at approximately 3×10^5 cells per well and cultured to 70–80% confluence. After the cells were starved in serum-free medium for 6 h, cell monolayers were scratched with a 200 μ l pipette tip and incubated in serum-free medium for 24 h. The wound sizes were recorded at 0 and 24 h. The wound closure percentage was calculated using the formula $(1 - [\text{final wound size}/\text{initial wound size}]) \times 100$.

2.8. Transwell assay

Cells were seeded into the upper chamber of a 24-well 8- μ m pore membrane (Corning, NY, USA) at 105 cells per cell. Approximately 500 μ l complete medium or serum-free medium containing FBS, 50 ng/ml FGF2, 100 nM AP24534 or 1 μ M ulixertinib was added to the lower chamber. After 24 h of incubation, cells in the upper chamber were removed, and cells in the bottom chamber were fixed with methanol and stained with crystal violet. Migrated cells were counted in 5 random visual fields of microscopy at $\times 200$ magnification.

2.9. Cell proliferation assays

Cell proliferation was detected by the cell counting kit-8 (CCK-8) assay and colony formation assay. Transfected cells were seeded in 96-well plates (5×10^3 /well) and incubated in serum-free medium for 6 h for starvation. Medium with 50 ng/ml FGF2, FBS, 100 nM AP24534 or 1 μ M ulixertinib was then added if necessary. Every 24 h, cells were mixed with 10 μ l CCK-8 (Dojindo, Tokyo, Japan) reagent per well and then incubated at 37 $^{\circ}$ C for 1 h. Then, the absorbance at 450 nm was measured. The relative OD450 was calculated as OD450 of tested well minus OD450 of empty medium.

For the colony formation assay, cells were seeded into 6-well plates (300/well) and complete medium for 2 weeks. After washing twice with phosphate-buffered saline (PBS), colonies were fixed with methanol and stained with crystal violet. The numbers of stained colonies were counted under a microscope.

2.10. Cell cycle detection

Cell cycle analysis was performed via fluorescence-activated cell sorting (FACS). A total of 3×10^5 cells were seeded in 6-well plates and cultured for 24–48 h in 50 ng/ml FGF2, FBS, 100 nM AP24534 and/or 1 μ M ulixertinib. After washing with PBS, the cells were harvested and fixed with cold 75% ethyl alcohol overnight at 4 $^{\circ}$ C. The cells were gently resuspended in 400–500 μ l propidium

iodide (PI)/RNase Staining solution (BD Biosciences, USA) at 37 °C for 15 min and incubated at 4 °C for 30 min in the dark. The samples were finally analyzed using a FACScan flow cytometer (BD Immunocytometry Systems, USA).

2.11. Apoptosis detection

Cell apoptosis assays were performed using a PE-Annexin V Apoptosis Detection Kit I (BD Biosciences, USA). In brief, 3×10^5 cells were seeded in 6-well plates and cultured for 24–48 h in 50 ng/ml FGF2, FBS, 100 nM AP24534 and/or 1 μ M ulixertinib. Cells were washed with PBS and resuspended in 400 μ l binding buffer. After incubation in 5 μ l PE-AnnexinV and 5 μ l 7-AAD for 15 min at 25 °C in the dark, the cells were mixed with 400 μ l binding buffer and analyzed by a FACScan flow cytometer within 1 h.

2.12. Tumor xenograft model

Female BALB/c nude mice (5–6 weeks old) from GemPharmatech Co., Ltd. (Nanjing, China) were randomly divided into two groups. Approximately 106 stable cells transfected with shSPRY4 or scrambled shRNA were subcutaneously injected into the right flanks of nude mice. Tumor diameters were measured every 3 days with a caliper. After euthanizing the mice and removing the xenografts, we calculated tumor volume as $(\text{length} \times \text{width}^2)/2$. Mice treated with AP24534 were given 10 mg/kg/day AP24534 via intraperitoneal injection. For FGF2 stimulation, mice treated with 3 mg/kg/day FGF2 via intraperitoneal injection. All animal experiments were supervised and approved by the Ethical Committee of Shandong University.

2.13. Statistical analysis

Statistical analyses were performed using SPSS 22.0 and GraphPadPrism 6.0 software. Data are presented as the mean \pm standard deviation. The statistical significance of differences between groups was calculated using Student's *t*-tests without special instruction. Correlations between SPRY4 expression and clinicopathological characteristics were determined by the Chi-square test or Fisher's test if necessary. Survival curves were estimated using the Kaplan–Meier method, and differences were assessed using the log-rank test. Multivariable analyses with the Cox proportional hazards regression model were used to determine independent prognostic factors. *P* value < 0.05 indicated statistical significance.

3. Results

3.1. Expression of different SPRY members in CCA

The mRNA levels of SPRY1–4 in tumors and paired tumor adjacent tissues from ICC (12 cases), PHCC (24 cases), and DCC (12 cases) patients were compared with qRT-PCR (Fig. 1(a)). Consistent with our previous results [29], the mRNA levels of SPRY2 in ICC tumor tissues were significantly lower than those in paired adjacent tissues. Intriguingly, PHCC exhibited different SPRY expression patterns than ICC. SPRY2 expression was not remarkably different between PHCC tumor and paired adjacent tissues, while the expression of SPRY1, SPRY3 and SPRY4 was notably lower in PHCC tumor tissues than in adjacent tissues (Fig. 1(b)), suggesting a potential tumor-suppressive role of SPRY1 and SPRY4 in PHCC. Moreover, we detected the expression of SPRY1–4 in 142 cases of PHCC with IHC and divided these cases into subgroups according to the H-scores of SPRY1–4 expression (Fig. 1(c)). All SPRY members were expressed in the cytoplasm instead of the nucleus. SPRY1 and 4 had relatively higher expression than SPRY2 and 3 in PHCC. Besides the PHCC cells, the mesenchymal cell of bile duct also had obvious SPRY4 staining, which was unlike SPRY1. In our

study, the proportions of high SPRY1–4 expression were 50.0%, 54.9%, 50.7%, and 50.0%, respectively (Supplemental Table 1).

3.2. Clinical significance of different SPRY members in CCA

The prognostic significance of SPRY1–4 and other clinicopathological factors in these 142 PHCC cases were first evaluated by univariate analysis Table 1. Among the four SPRY members, SPRY4 was the only marker of favorable prognosis in PHCC ($P = 0.006$) (Fig. 2(a)–(d)). In addition to SPRY4 expression, patient age > 65 ($P = 0.013$), positive lymph node metastasis ($P = 0.025$), positive metastasis ($P < 0.001$), and advanced TNM stage ($P < 0.001$) were all significantly associated with low survival rates in our study (Fig. 2(e)–(h)).

Independent prognostic biomarkers of PHCC were further identified with the Cox regression models (Supplemental Table 2). The prognostic factors identified in univariate analyses were included in a multivariate analysis except TNM stage because of its natural interaction with other factors. In our study, SPRY4 was confirmed as an independent biomarker predicting a favorable prognosis in PHCC.

To identify the possible processes underlying tumor progression affected by SPRY4, we analyzed its correlation with clinicopathological factors, including lymphatic invasion, metastasis, and tumor differentiation (Supplemental Table 3). In our study, high expression of SPRY4 was significantly associated with small tumor size ($P = 0.007$), negative lymphatic invasion ($P = 0.031$) and early TNM stage ($P = 0.002$), indicating that SPRY4 may suppress the proliferation and invasion of PHCC. In addition, we analyzed the correlations between SPRY1–3 and clinicopathological factors. Interestingly, the expression levels of SPRY1 and SPRY2 were correlated with tumor size (Supplemental Table 4).

3.3. SPRY4 expression can be induced by ectopic FGFR2 activation in PHCC

As a modulator of ERK phosphorylation, SPRY expression was previously reported to be induced by ERK activation as a negative feedback [13]. However, the expression of both FGFR and SPRY4 family was context- and tissue-specific, so we further detected the correlations between SPRY4 and FGFR family. The expression of FGFR1–4 was detected with IHC and divided into low and high expression (Fig. 3(a)). High expression of FGFR4 was a prognostic biomarker of PHCC, which was in consistent with our previous study [35]. Besides FGFR4, high expression of FGFR2 also indicated poor prognosis of PHCC (Fig. 3(b)). Among FGFR1–4, the expression of FGFR2 had most significant correlation with SPRY4 expression ($R^2 = 0.468$) (Fig. 3(c)), and patients with high FGFR2 seemed to have higher expression of SPRY4 (Fig. 3(d)). PHCC cell line QBC939 was incubated in 10 ng/ml FGF2 for 0–72 h. In this long-term activation, SPRY4 expression was elevated by FGF2 (Fig. 3(e)), indicating that SPRY4 expression could be induced in ectopic activation of FGFR2.

3.4. SPRY4 inhibited the proliferation and invasion of PHCC

The role of SPRY4 in PHCC progression was further evaluated through *in vitro* and *in vivo* experiments. The expression of SPRY4 in 8 pairs of fresh PHCC tissues and corresponding tumor adjacent tissues was detected by western blotting, which indicated lower expression of SPRY4 in PHCC (Fig. 4(a)). Moreover, SPRY4 expression was detected in ICC cell lines RBE and HCCC-9810 and PHCC cell lines FRH0201 and QBC939 (Fig. 4(b)). SPRY4 expression was detectable in all these cell lines and was most prominent in QBC939 cells. After silencing SPRY4 with shRNAs in QBC939 and overexpressing SPRY4 in FRH0201 with lentivirus carrying LV5-SPRY4 (Fig. 4(c)), we evaluated the proliferation and migration of QBC939 cells. Both CCK-8 and colony formation assays showed that SPRY4 knockdown substantially promoted the proliferation of QBC939 cells (Fig. 4(d) and (e)), and SPRY4 overexpression facilitated the progression of FRH0201 cells (Fig. 4(d) and (e)). Similar

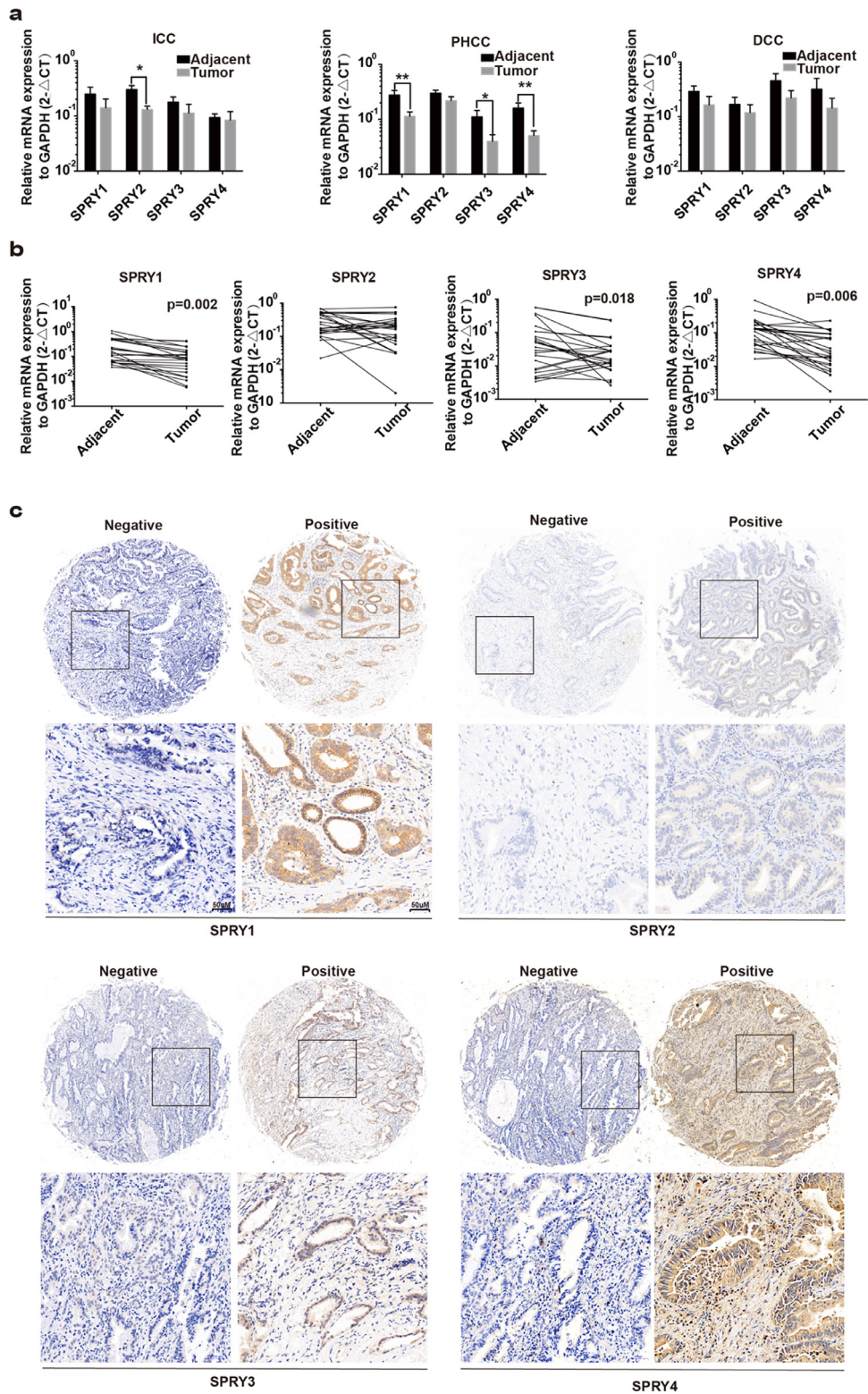


Fig. 1. Expression of SPRY family members in ICC, PHCC, DCC and adjacent normal tissues. (a) Relative mRNA levels of SPRY family members in ICC ($n = 12$), PHCC ($n = 24$) and DCC ($n = 12$) tissues and adjacent normal tissues were detected by qRT-PCR. Results were analyzed using the $2^{-\Delta\Delta CT}$ method with GAPDH as an internal control. * and ** represent $P < 0.05$ and $P < 0.01$, respectively, calculated by paired t -test between the indicated subgroups. (b) Relative mRNA levels of SPRY family members between PHCC tumor and adjacent tissues ($n = 24$) compared with paired t -tests. Results were analyzed using the $2^{-\Delta\Delta CT}$ method with GAPDH as an internal control. Results were analyzed with paired t -test. (c) Representative IHC images of SPRY family members in human PHCC tissues. Scale bar: 50 μ m.

results were obtained in transwell and wound healing assays, suggesting that SPRY4 also played an essential role in the migration of QBC939 cells (Fig. 4f and (g)). In addition, stable QBC939 cells with SPRY4 knockdown were established and subcutaneously transplanted into

nude mice for successful xenograft formation (Fig. 4(h)). Consequently, SPRY4 knockdown resulted in an increase in the volume and weight of xenografts (Fig. 4(i) and (j)), indicating the important tumor-suppressive role of SPRY4 in PHCC cell proliferation.

Table 1
Prognostic significance of clinicopathological factors.

Clinicopathological factors	3-year OS rate	P*
Sex		
Male	43.9	0.611
Female	25.4	
Age (y)		
< 65	44.7	0.013
≥ 65	23.9	
Tumor size		
< 3cm	42.5	0.053
≥ 3cm	29.7	
Differentiation		
Well	38.5	0.360
Moderate+poor	35.8	
T stage		
T1	61.0	0.702
T2+T3+T4	35.1	
N stage		
N0	43.9	0.025
N1+N2	22.9	
M stage		
M0	37.3	<0.001
M1	0	
TNM stage		
I+II	48.6	<0.001
III+IV	21	
SPRY1 expression		
low	37.7	0.953
high	32.7	
SPRY2 expression		
low	39.3	0.759
high	33.1	
SPRY3 expression		
low	33.9	0.876
high	40.7	
SPRY4 expression		
low	20.9	0.006
high	46.6	

* Calculated with log-rank test.

3.5. *SPRY4* suppressed *FGF2*-induced *PHCC* progression

SPRY4 was reported to block *ERK* activation induced by several upstream stimulators, including *FGFR* and *EGFR* [36]. Additionally, *FGFR2* is a well-known biomarker of *CCA*. Thus, we determined the role of *SPRY4* in *FGF2*-induced *PHCC* progression. After *SPRY4* knock-down, *QBC939* cells were serum-starved for 6 h and incubated in 50 ng/ml *FGF2* and 1% *FBS* for 1–4 days. Consequently, *SPRY4* silencing significantly increased *FGF2*-induced proliferation of *QBC939* cells (Fig. 5(a)). Moreover, a pan-inhibitor of *FGFR*, *AP24534* (100 nM), was used to block *FGFR* signaling. As expected, the *FGFR* inhibitor *AP24534* remarkably decreased *FGF2*-induced proliferation, while *SPRY4* knockdown substantially attenuated this effect (Fig. 5 (b)). Transwell assays were also performed in the presence of 50 ng/ml *FGF2* and 5% *FBS*. *AP24534* significantly suppressed the migration of *QBC939* cells induced by *FGF2*, whereas the migration of *QBC939* cells enhanced by *SPRY4* knockdown (Fig. 5(c)). These *in vitro* results demonstrated that *SPRY4* knockdown could enhance *FGF2*-induced *PHCC* cell proliferation and migration, suggesting that *SPRY4* was essential for suppressing *FGF2*-induced *PHCC* progression.

Next, *in vivo* experiments were carried out to confirm the tumor-suppressive role of *SPRY4*. Nude mice were intraperitoneally injected with *AP24534* at a dose of 10 mg/kg/day for 15 days after being inoculated with stable *SPRY4*-knockdown *QBC939* cells (Fig. 5(d)). Mice injected with *AP24534* had significantly smaller tumor volumes and lower tumor weights (Fig. 5(e) and (f)), indicating that the *FGFR* inhibitor could block the proliferation promoted by *SPRY4* knock-down.

3.6. *SPRY4* suppressed *FGF2*-induced *ERK* phosphorylation

ERK is the main downstream effector of *FGF-FGFR2* signaling, and we previously proved that *SPRY2* could suppress *ERK* phosphorylation in *ICC* cells. Thus, we further detected the function of

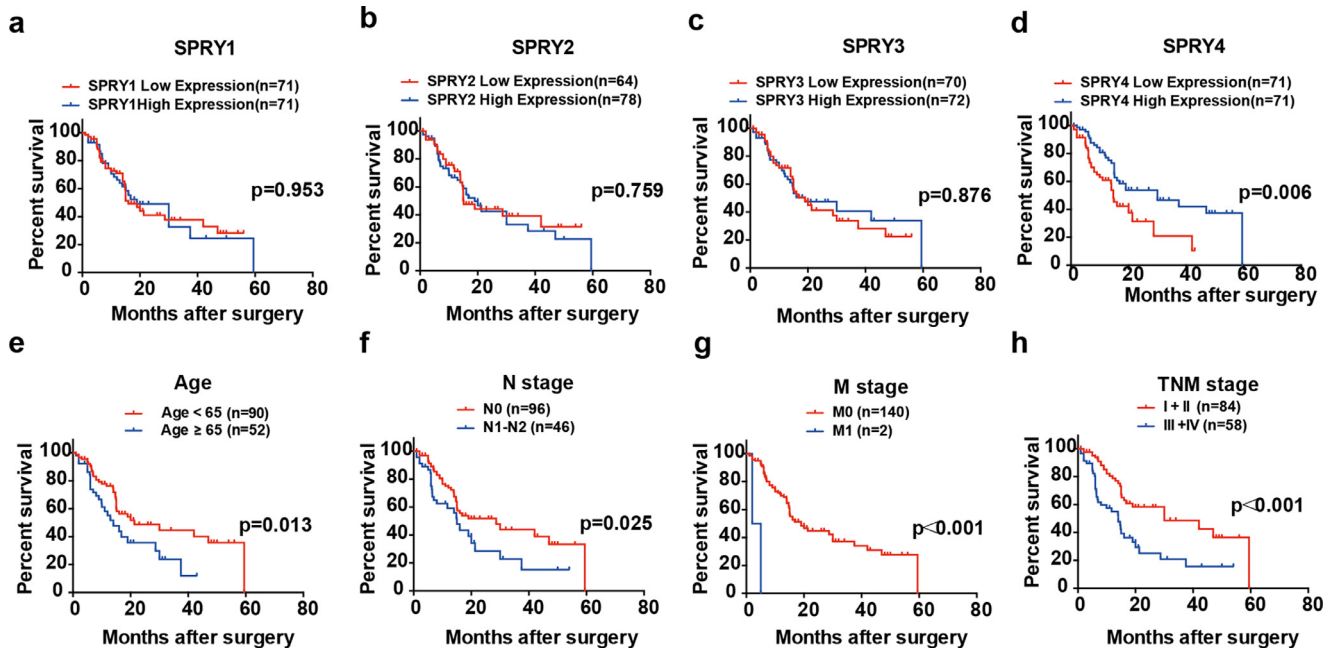


Fig. 2. Correlation between overall survival rates, *SPRY* members and clinicopathological factors. (a)–(c) Expression of *SPRY1* (a), *SPRY2* (b) and *SPRY3* (c) displayed no prognostic significance. (d) Low expression of *SPRY4* was significantly correlated with low overall survival rates in *PHCC* patients. (e)–(h) Advanced patient age (e), positive lymph node metastasis (f), positive distant metastasis (g) and advanced *TNM* stage (h) were all associated with poor prognosis. Results were analyzed using the Kaplan–Meier method, and the statistical significance between groups was assessed using the log-rank test.

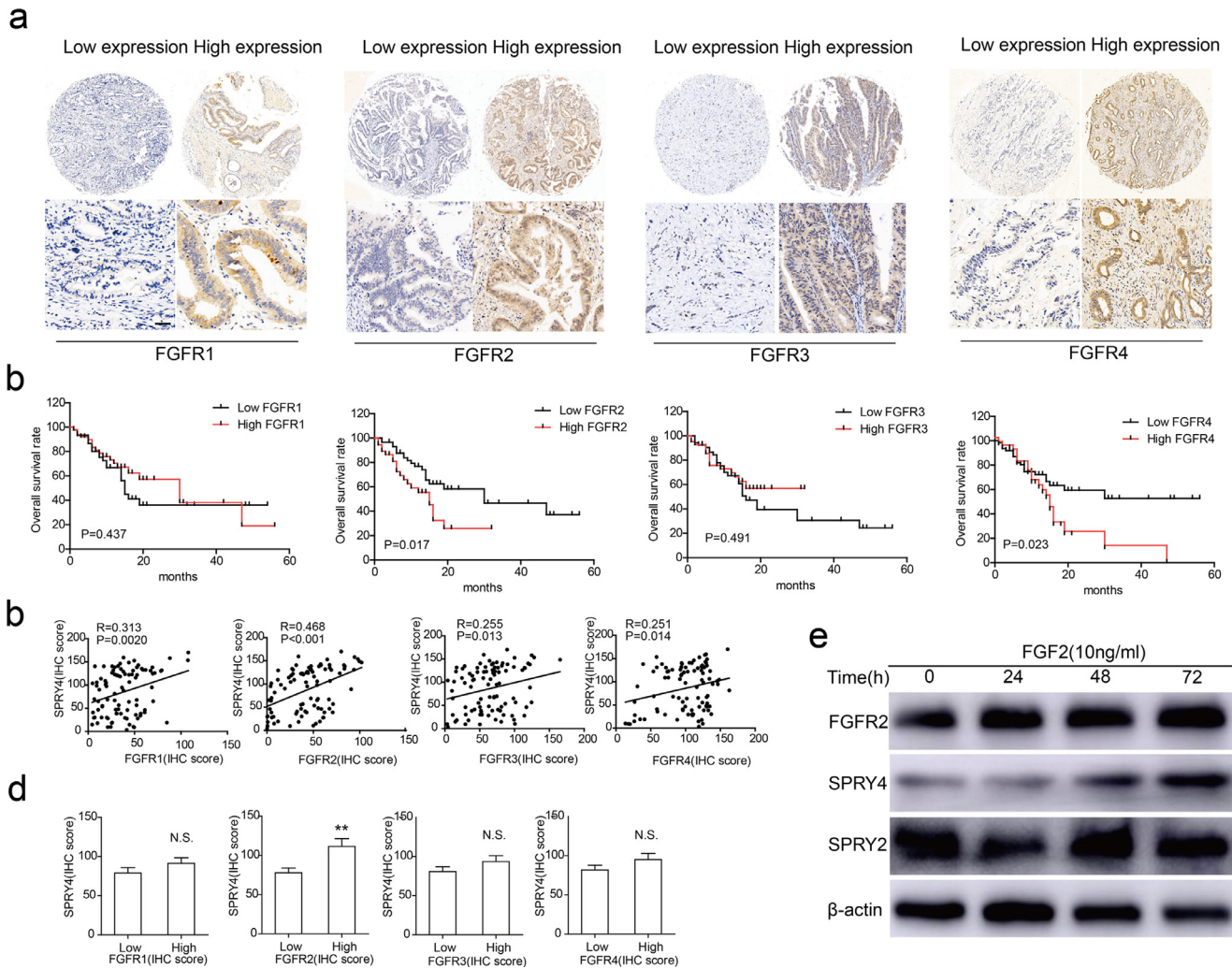


Fig. 3. SPRY4 expression was associated with FGFR2 in PHCC (a) Representative IHC images of FGFR family members in human PHCC tissues. Scale bar: 50 μ m. (b) Correlations between overall survival rates and FGFR members in PHCC patients. The statistical significance between groups was assessed using the log-rank test. (c) The correlation of IHC score between SPRY4 expression and FGFR family. The linear regression was analyzed with Pearson method. (d) The IHC score of SPRY4 in patients with low and high expression of FGFR members. *P* value was analyzed with student's *t*-test.

SPRY in FGF2-induced ERK phosphorylation. SPRY4 silencing was shown to enhance ERK phosphorylation of QBC939 cells in 10% FBS (Fig. 6(a)). Next, the time-effect correlation between FGF2 and ERK phosphorylation was evaluated. QBC939 cells displayed peak ERK phosphorylation levels after 5 min of stimulation with 50 ng/ml FGF2 (Fig. 6(b)). This FGF2-induced ERK phosphorylation was antagonized by AP24534 and enhanced by SPRY4 silencing in QBC939 cells (Fig. 6(c)), consistent with FGF2-induced PHCC progression.

The ERK inhibitor ulixertinib was next used in the presence of FGF2 stimulation. To this end, QBC939 cells were incubated with ulixertinib (1 μ M) and FGF2 (50 ng/ml), and PHCC cell proliferation and migration were detected. Both CCK-8 and transwell assays revealed that ERK inhibition could suppress the promotion of proliferation and migration induced by SPRY4 knockdown (Fig. 6(d) and (e)). These results suggested that ERK activation was essential in the SPRY4-induced suppression of PHCC progression. Moreover, *in vivo* experiments were conducted with SPRY4-overexpressing QBC939 cells, with or without FGF2 stimulation (Fig. 6(f)). SPRY4 overexpression repressed tumor volume and weight, while recombinant FGF2 stimulation reversed this tendency (Fig. 6(g) and (h)), indicating SPRY4 was an essential modulator of FGF-FGFR4-ERK signaling pathway.

3.7. SPRY4 arrested the cell cycle in the G1 phase by inhibiting ERK activation and decreasing Cyclin D1 expression

In the clinical analysis of supplemental Table 3, we observed that SPRY4 was significantly associated with tumor size. Moreover, *in vitro* and *in vivo* experiments, SPRY4 was shown to suppress tumor proliferation. Therefore, we determined whether SPRY4 influenced apoptosis in PHCC cells. After stimulation with FGF2, flow cytometry was used to identify apoptotic cells after SPRY4 knockdown (Fig. 7(a)), and apoptosis biomarkers including Bax, Bcl-2 and Caspase-3 were also detected by western blotting (Fig. 7(b)). However, apoptosis in QBC939 cells was not markedly different between the shSPRY4- and scrambled shRNA-transfected groups, suggesting that SPRY4 did not affect apoptosis in QBC939 cells.

The effect of SPRY4 on the cell cycle of QBC939 cells was subsequently evaluated by flow cytometry with PI staining. FGF2 stimulation at 50 ng/ml reduced the percentage of QBC939 cells in the G1 phase (Fig. 7(c)). Furthermore, the cell cycle of QBC939 cells was detected in the presence or absence of AP24534 after SPRY4 silencing. SPRY4 knockdown substantially decreased the proportion of cells in the S and G2/M phase, while AP24534 attenuated this effect (Fig. 7(d)). These results suggested that SPRY4 could suppress FGF-induced

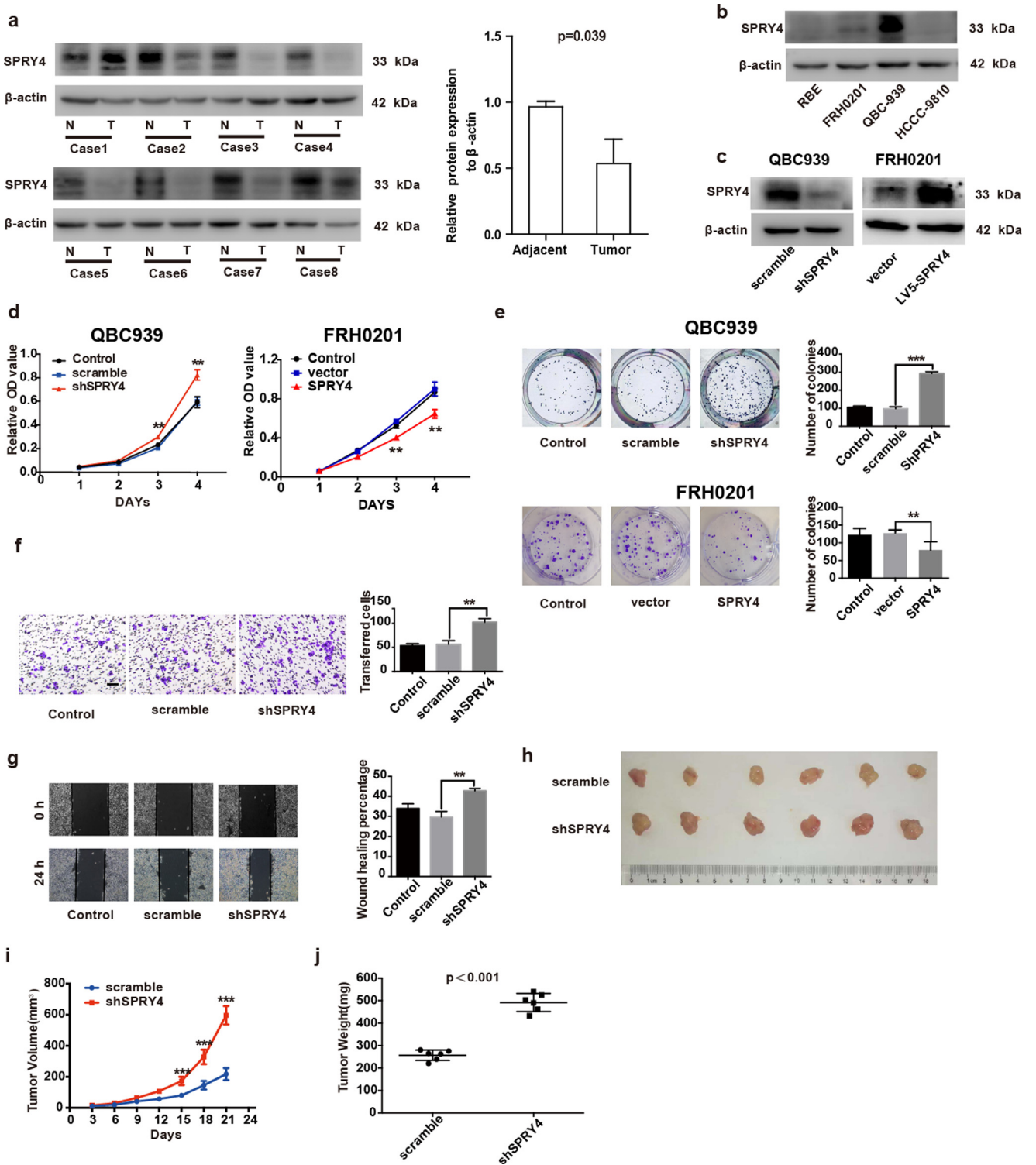


Fig. 4. SPRY4 suppressed the proliferation and migration of PHCC cells. (a) Left: SPRY4 protein expression in 8 pairs of PHCC and adjacent tissues were detected by western blotting. Right: quantification of western blots. Results were analyzed with paired *t*-test and shown with \pm S.D. (b) SPRY4 expression was detected in ICC cell lines RBE and HCCC-9810, and PHCC cell lines QBC939 and FRH0201. (c) Knockdown of SPRY4 in QBC939 cells, and overexpression of SPRY4 in FRH0201 cells with lentivirus infection was verified by western blotting. (d) and (e) Proliferation of QBC939 cells was detected with CCK-8 (d) and colony formation assays (e) after silencing SPRY4 in QBC939 cells and overexpressing SPRY4 in FRH0201 cells in normal medium with 10% FBS. (f) and (g) Migration of QBC939 cells was assessed with transwell assay (g). After SPRY4 knockdown, cells were seeded in the upper transwell chamber and incubated for 24 h, with FBS in the lower chamber. (g) Wound healing assay was applied to evaluate migration of QBC939. 24 h after a scratch in the cell monolayer, the wound size was measured again. Wound closure percentage was calculated by $(1 - [\text{final wound size} / \text{initial wound size}]) \times 100$. In d, e, f and g, ** and *** represented $P < 0.01$ and $P < 0.001$ by Student *t*-test, between scrambled/vector groups and SPRY4-overexpressing/silencing groups (h) Xenografts were established in nude mice with stable QBC939 cells with SPRY4 knockdown or control cells. (i) and (j) SPRY4 knockdown increased the volume(i) and weight (j) of xenograft tumors. Tumor diameter was measured every 3 days. In d, e, f, g, i and j, ** and *** represented $P < 0.01$ and $P < 0.001$ by Student's *t*-test, between the indicated groups.

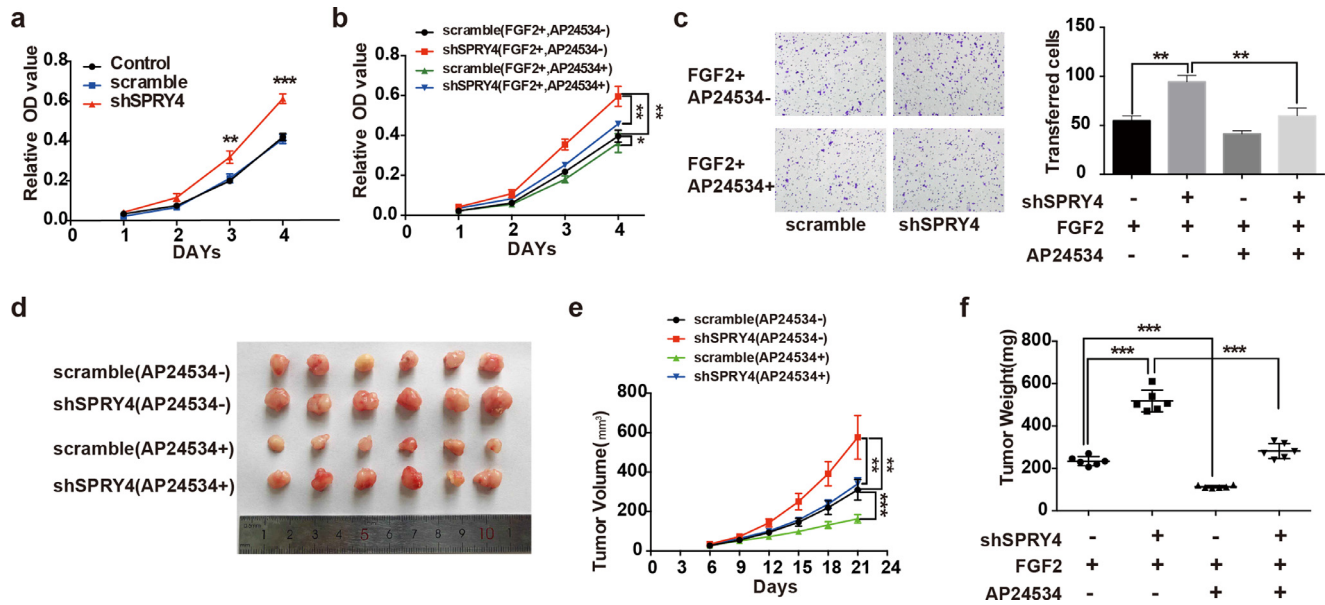


Fig. 5. Down-regulation of SPRY4 expression promoted FGF2-mediated proliferation and migration. (a) Proliferation of QBC939 cells was measured with CCK-8 assay in medium containing FGF2 (50 ng/ml) and 1% FBS after SPRY4 knockdown. (b) After starvation in serum-free medium for 6 h, QBC939 cells were incubated with FGF2 (50 ng/ml), 1% FBS and/or 100 nM AP24534 for 1–4 days, and cell proliferation was detected with CCK-8 assay. (c) Left panel: representative images of migrated cells with/without 100 nM AP24534 for 24 h. Lower chamber contained 50 ng/ml FGF2 and 5% FBS. Right: statistical analysis of cells undergoing different stimulation. (d) Xenografts were established in nude mice with stable QBC939 cells infected with shSPRY4 or scrambled shRNA in the presence or absence of AP24534 at 10 mg/kg/day via intraperitoneal injection. (e and f) AP24534 decreased the volume and weight of xenograft tumors, which had been promoted by SPRY4 knockdown. In a, c, e and f, *, ** and *** represent $P < 0.05$, $P < 0.01$ and $P < 0.001$, respectively. The statistical significance was analyzed with Student's t-tests or one-way ANOVA.

proliferation by arresting cells in the G1 phase. In addition, cell cycle proteins, including Cyclin A2, Cyclin B1 and Cyclin D1, were also detected by western blotting (Fig. 7(e)). SPRY4 knockdown promoted the expression of Cyclin D1 but not Cyclin A2 or B1, and AP24534 decreased Cyclin D1 expression, indicating that SPRY4 knockdown increased the proportion of S and G2/M phase cells by promoting Cyclin D1 expression. The ERK inhibitor ulixertinib had a similar effect as AP24534 on cell cycle distribution (Fig. 7(f)) and cell cycle-related protein expression (Fig. 7(g)), indicating that ERK was the main downstream effector of the SPRY4-induced effect on the cell cycle of QBC939 cells. The levels of cell cycle proteins were also detected in xenograft models. Cyclin D1 expression was increased in tumors with SPRY4 knockdown (Fig. 7(h) and (i)) and decreased in response to AP24534 treatment (Fig. 7(j)), further confirming that SPRY4 could attenuate proliferation by arresting the cell cycle in the G1 phase.

4. Discussion

CCA is a highly heterogeneous and aggressive malignancy with a dismal prognosis. For a very long time, CCA was divided into intrahepatic and extrahepatic CCA, and the latter type included both PHCC and DCC. In 2007, the 7th AJCC/UICC system separated PHCC as a distinct subtype of CCA for the first time [37], and thus the biomarker study of PHCC started very late. Moreover, the biological differences between PHCC and DCC have rarely been investigated. High-throughput analyses have indicated several molecular differences between the two subtypes, but few functional and clinical studies have been performed to verify these differences. Radical surgery is very difficult in PHCC because most patients present with advanced stages, which prevent an R0 surgical margin. In addition, perihilar surgery is one of the most complicated hepatobiliary surgeries, and no consensus has been reached for the standard surgical method for PHCC [4]. All of these reasons attributed to the fact that PHCC cohorts are difficult to collect, and therefore, the biomarker study of PHCC remains stagnant. In our study, 142 patients were enrolled, representing the largest

cohort of PHCC cases to the best of our knowledge. For the first time, we investigated the expression of SPRY family members in different types of CCA and found that SPRY4 was an independent biomarker of PHCC but not of DCC. This conclusion also supports that PHCC and DCC have different molecular characteristics. In our previous report [29], we demonstrated that among the SPRY family members, only SPRY2 can indicate a favorable prognosis in ICC. Combined with the results in this study, we proved that the tissue specificity of SPRY family members was very obvious in CCA and suggested that different SPRY members may have different expression patterns or functions in distinct tumor types or tumor progression periods.

The prognosis of PHCC patients is very dismal. A main reason for this grim prognosis is that the effect of adjuvant therapy of PHCC is very limited. Unfortunately, no targeted drugs are available for PHCC, and a lower number of potential drugs are in clinical trials for PHCC than that for other tumors. Targeted therapy and precise treatment of PHCC require much more attention because of its increasing incidence and poor prognosis. In our study, for the first time, we demonstrated that SPRY4 expression was correlated with progression and poor prognosis in PHCC and that SPRY4 suppressed cell proliferation by arresting the cell cycle in the G1 phase. Moreover, we demonstrated that the inhibition of ERK phosphorylation was the main mechanism underlying SPRY4-mediated regulation of cell cycle and proliferation. Our findings could provide more insights into the tumor-suppressive function of SPRY4. The molecular mechanism by which SPRY4 inhibits ERK phosphorylation is still controversial. Different studies have shown that SPRY can suppress ERK activation at multiple upstream levels, including inhibiting Grb2, RAS or Raf activity [36,15], but this was not well elucidated in our study. We hope that our discovery of the clinical significance of SPRY4 could spark more interest regarding the underlying mechanism of how SPRY4 regulates ERK phosphorylation.

As the most important negative modulator of FGFR-ERK signaling, SPRY expression was reported to be elevated by continuous ERK activation [29], which in turn suppresses the ERK phosphorylation. This was also proved by our results that long-term FGF2 stimulation promoted the expression of SPRY4 in PHCC cells. However, short-term

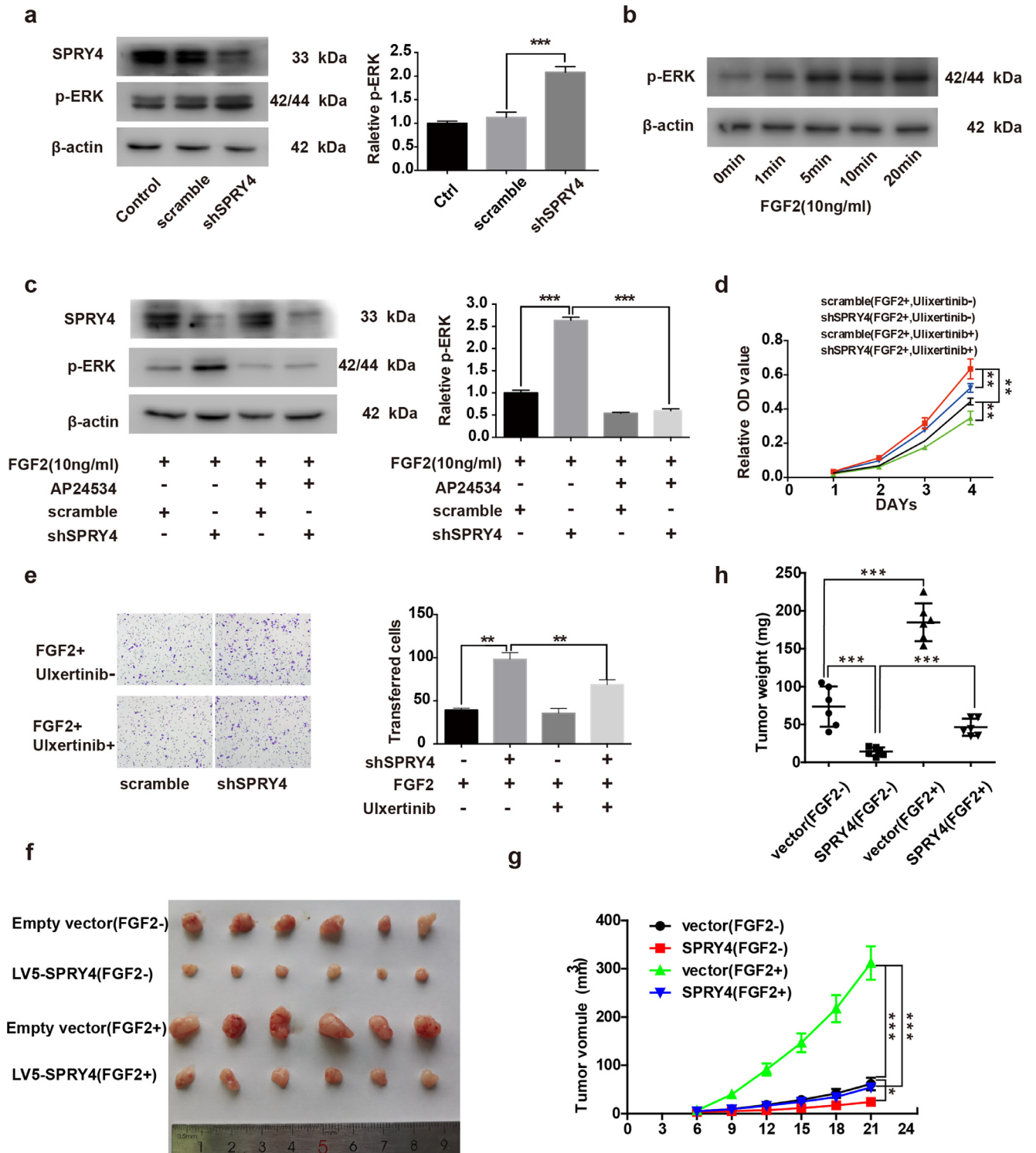


Fig. 6. SPRY4 knockdown promoted the progression of PHCC by enhancing FGF2-mediated ERK phosphorylation. (a) Left: SPRY4 expression was silenced, and ERK phosphorylation was detected with western blotting. Right: quantification of p-ERK expression in the left panel. (b) ERK phosphorylation in QBC939 cells peaked after 5 min of stimulation of 10 ng/ml FGF2. (c) Left: the FGFR inhibitor AP24534 antagonized ERK phosphorylation induced by SPRY4 knockdown. QBC939 cells were incubated in serum-free medium with AP24534 (100 nM) for 6 h and then stimulated with FGF2 (10 ng/ml) for 10 minutes. Right: quantification of p-ERK levels in the left panel. (d) Proliferation was detected after QBC939 cells were starved in serum-free medium for 6 h and cultured in medium containing 50 ng/ml FGF2 and 1%FBS, in the presence or absence of 100 nM ulixertinib. (e) QBC939 cells were starved and incubated with 1 μM ulixertinib and 50 ng/ml FGF2 for 24 h. Left: representative images of migrated cells. Right: statistical analysis of cells undergoing different stimulation. (f) SPRY4-overexpressing QBC939 cells were injected subcutaneously for xenografts with 3 mg/kg/day FGF2 via intraperitoneal injection. (g) and (h) SPRY4 overexpression decreased tumor volume and weight, while FGF2 addition reversed the effect. In a, c, d, e, g and h, ** and *** represent $P < 0.01$ and $P < 0.001$, respectively, between the indicated subgroups. The significance was calculated by Student's *t*-test.

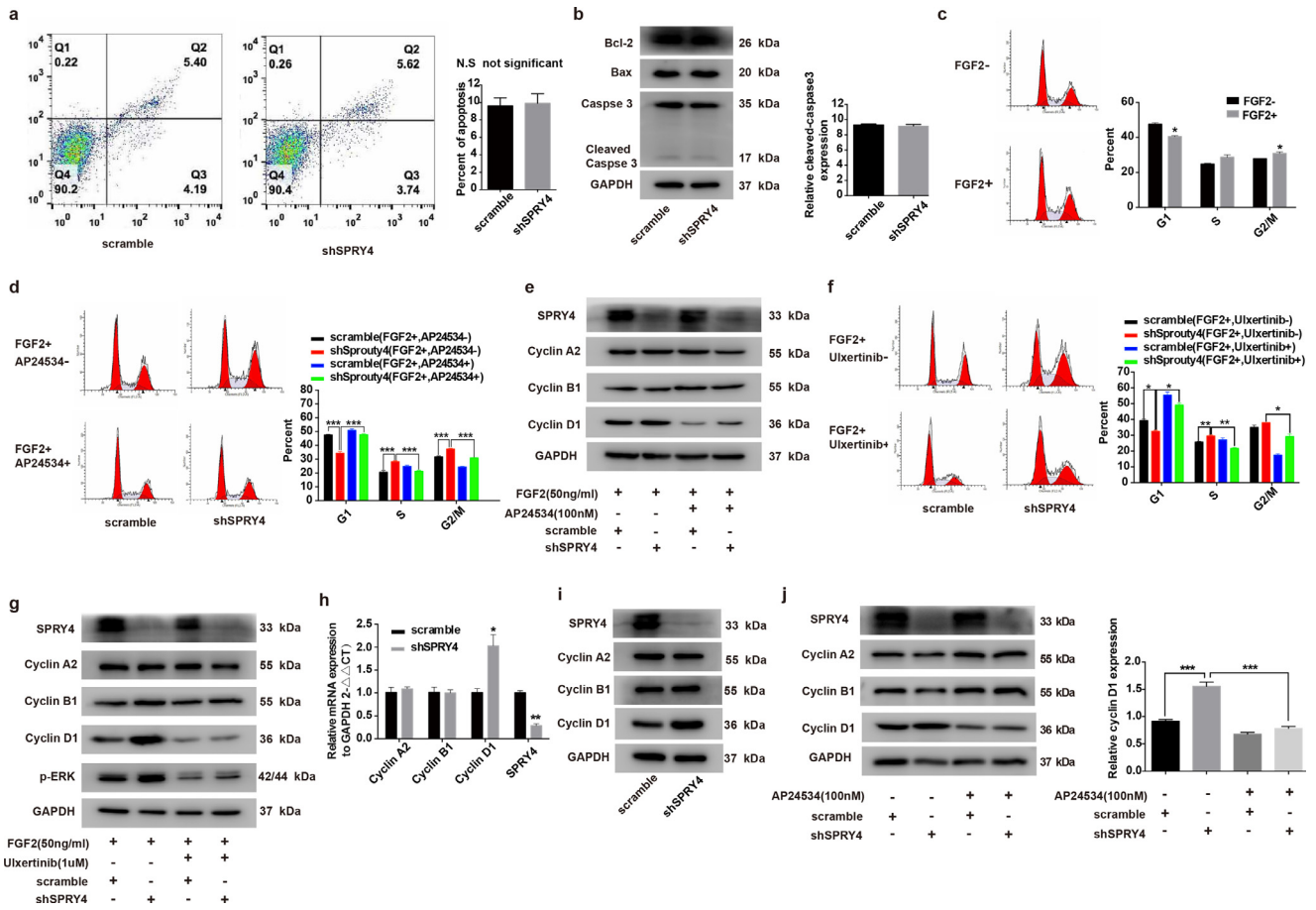


Fig. 7. SPRY4 arrested PHCC cells in the G1 phase by decreasing Cyclin D1 expression. (a) SPRY4 expression did not influence apoptosis in QBC939 in response to 50 ng/ml FGF2. Left: representative images of apoptotic cells detected using flow cytometry. Right: proportions of apoptotic cells. (b) SPRY4 expression had no effect on the expression of BAX, Bcl-2 and Caspase-3. Left: expression levels of BAX, Bcl-2, Caspase-3 and cleavage Caspase-3 were detected by western blotting after SPRY4 knockdown and 50 ng/ml FGF2 stimulation. Right: quantification of cleaved Caspase-3 in QBC939 cells. In A and B, N.S. represents not significant. (c) Left: proportions of QBC939 cells in different phases of the cell cycle detected using flow cytometry in the presence of 50 ng/ml FGF2. Right: FGF2 stimulation decreased the proportion of cells in the G1 phase. (d) Left: proportions of QBC939 cells in different phases of the cell cycle were detected in the presence of 50 ng/ml FGF2 and/or 100 nM AP24534. Right: proportion of cells in the G1 phase was decreased by SPRY4 knockdown and increased by 100 nM AP24534 incubation, and that of cells in the S and G2/M phases displayed the opposite tendency. (e) Expression levels of Cyclin A2, B1 and D1 in QBC939 cells were detected with/without AP24534 incubation after SPRY4 knockdown. (f) Left: QBC939 cells were incubated in 1 μM ulixertinib for 24 h, and the cell cycle distribution was detected. Right: ulixertinib increased the percentage of cells in the G1 phase and decreased the percentage of cells in the S and G2/M phases. (g) Expression levels of Cyclin A2, B1 and D1 in QBC939 cells were detected after incubation in 1 μM ulixertinib for 24 h. (h) and (i) mRNA (h) and protein (i) levels of cell cycle-related proteins in subcutaneous xenograft tumors established with stable SPRY4 knockdown cells were detected using qRT-PCR and western blotting. (j) Left: levels of cell cycle-related proteins in subcutaneous xenograft tumors treated with AP24534 were detected. Right: Cyclin D1 expression was increased by SPRY4 knockdown and decreased by AP24534 treatment. In D, F, H and J, *, ** and *** represent $P < 0.05$, $P < 0.01$ and $P < 0.001$, respectively, between the indicated subgroups. Significance was calculated with Student's t-test.

stimulation like FGFR2 inhibitor had no obvious effect on SPRY4 expression. This SPRY4 feedback may be a protective mechanism of cells to maintain the proper activation of ERK. SPRY4 down-regulation as well as FGFR2 overexpression of tumor cells broke this balance and resulted in the proliferation out of control. FGFR2 expression had significant association with SPRY4, but FGFR2 high expression indicated poor prognosis while SPRY4 was associated with favorable prognosis of PHCC. This indicated that SPRY4 function can be up-regulated by FGFR2 stimulation and furthermore balance out the FGFR2-induced progression to some extent, pointing the potential therapeutic significance of SPRY4 in PHCC.

RAS mutations and FGFR2 fusions are the most well-accepted molecular features of CCA8. These genetic alterations lead to conformation changes and constitutive activation of the corresponding proteins [38]. Constitutive activation of these proteins eventually stimulates downstream signals, and ERK is a common effector of RAS and FGFR2 signaling. Several inhibitors of RAS and FGFR2 are currently in clinical trials or preclinical studies [39], but it is uncertain whether these trials would bring out new target drugs. Furthermore, a recent study showed that tumor cells may develop FGFR2 mutations

and exhibit resistance to FGFR2 inhibitors [40]. Our findings that SPRY4 inhibits ERK activation in PHCC indicated that SPRY4 could also be a potential therapeutic target. Drugs activating SPRY4 function can theoretically inhibit ERK activation and suppress tumor progression. This may provide new strategies for inhibiting FGFR2 or RAS signaling because most target drugs are small molecular inhibitors or monoclonal antibodies, and few of these drugs are agonists.

In conclusion, for the first time, we compared the expression of all the SPRY family members in different subtypes of CCA and investigated their prognostic significance in PHCC. Consequently, we demonstrated that SPRY4 was notably associated with tumor size and lymphatic invasion and that it was an independent prognostic biomarker of PHCC. In PHCC, SPRY4 expression was significantly associated with FGFR2 expression and its expression could be induced by ectopic activation of FGFR2. Through *in vitro* and *in vivo* experiments, we demonstrated that SPRY4 can suppress FGFR-induced proliferation and migration of PHCC cells by inhibiting ERK phosphorylation. Furthermore, we revealed that SPRY4 inhibited proliferation by arresting cells in the G1 phase and by reducing Cyclin D1 expression. Our results indicated that SPRY4 may be a potential target for PHCC

treatment and suggested that the detection of SPRY4 in PHCC patients can help stratify high- and low-risk patients more effectively, which may guide individualized therapy for PHCC.

Declaration of Competing Interest

The authors declare no conflicts of interest.

Acknowledgments

Our study was supported by National Natural Science Foundation of China (Grant no. 81601668), Shandong Province Major Research and Design Program (Grant no. 2018GSF118169), Natural Science Foundation of Shandong (ZR2019MH008), Jinan City Science and Technology Development Program (Grant no. 201805017, 201805013), Hengrui Hepatobiliary and Pancreatic Foundation (Grant no. Y-2017-144), and Sciclone Clinical oncology research foundation (Y-2019Sci-clone-001). The funders had no role in study design, data collection, data analysis, interpretation, writing of the report.

Supplementary materials

Supplementary material associated with this article can be found, in the online version, at doi:10.1016/j.ebiom.2019.11.021.

Reference

- [1] Razumilava N, Gores GJ. Cholangiocarcinoma. *Lancet* 2014;383(9935):2168–79 Epub 2014/03/04.
- [2] Witjes CD, Karim-Kos HE, Visser O, de Vries E, JN IJ, de Man RA, et al. Intrahepatic cholangiocarcinoma in a low endemic area: rising incidence and improved survival. *HPB: Off J Int Hepato Pancreato Biliary Assoc* 2012;14(11):777–81 Epub 2012/10/10.
- [3] DeOliveira ML, Cunningham SC, Cameron JL, Kamangar F, Winter JM, Lillemoie KD, et al. Cholangiocarcinoma: thirty-one-year experience with 564 patients at a single institution. *Ann Surg* 2007;245(5):755–62 Epub 2007/04/26.
- [4] Xu YF, Liu ZL, Pan C, Yang XQ, Ning SL, Liu HD, et al. HMGBl correlates with angiogenesis and poor prognosis of perihilar cholangiocarcinoma via elevating VEGFR2 of vessel endothelium. *Oncogene* 2019;38(6):868–80 Epub 2018/09/05.
- [5] Squadroni M, Tondulli L, Gatta G, Mosconi S, Beretta G, Labianca R. Cholangiocarcinoma. *Crit Rev Oncol Hematol* 2017;116:11–31 Epub 2017/07/12.
- [6] Valle JW. Advances in the treatment of metastatic or unresectable biliary tract cancer. *Ann Oncol: Off J Eur Soc Med Oncol/ESMO* 2010;21(Suppl 7):vii345–8 Epub 2010/10/15.
- [7] Nakamura H, Arai Y, Totoki Y, Shirota T, Elzawahry A, Kato M, et al. Genomic spectra of biliary tract cancer. *Nat Genet* 2015;47(9):1003–10 Epub 2015/08/11.
- [8] Ong CK, Subimerb C, Pairojikul C, Wongkham S, Cutcutache I, Yu W, et al. Exome sequencing of liver fluke-associated cholangiocarcinoma. *Nat Genet* 2012;44(6):690–3 Epub 2012/05/09.
- [9] Sia D, Losic B, Moeini A, Cabellos L, Hao K, Revill K, et al. Massive parallel sequencing uncovers actionable FGFR2-PPHLN1 fusion and ARAF mutations in intrahepatic cholangiocarcinoma. *Nat Commun* 2015;6:6087. Epub 2015/01/23.
- [10] Arai Y, Totoki Y, Hosoda F, Shirota T, Hama N, Nakamura H, et al. Fibroblast growth factor receptor 2 tyrosine kinase fusions define a unique molecular subtype of cholangiocarcinoma. *Hepatology* 2014;59(4):1427–34 Epub 2013/10/15.
- [11] Wu YM, Su F, Kalyana-Sundaram S, Khazanov N, Ateeq B, Cao X, et al. Identification of targetable FGFR gene fusions in diverse cancers. *Cancer Discov* 2013;3(6):636–47 Epub 2013/04/06.
- [12] Wang Y, Ding X, Wang S, Moser CD, Shaleh HM, Mohamed EA, et al. Antitumor effect of FGFR inhibitors on a novel cholangiocarcinoma patient derived xenograft mouse model endogenously expressing an FGFR2-CCDC6 fusion protein. *Cancer Lett* 2016;380(1):163–73 Epub 2016/05/25.
- [13] Masoumi-Moghaddam S, Amini A, Morris DL. The developing story of Sprouty and cancer. *Cancer Metastasis Rev* 2014;33(2–3):695–720 Epub 2014/04/20.
- [14] Hanafusa H, Torii S, Yasunaga T, Nishida E. Sprouty1 and Sprouty2 provide a control mechanism for the RAS/MAPK signalling pathway. *Nat Cell Biol* 2002;4(11):850–8 Epub 2002/10/29.
- [15] Yusoff P, Lao DH, Ong SH, Wong ES, Lim J, Lo TL, et al. Sprouty2 inhibits the RAS/MAP kinase pathway by inhibiting the activation of RAF. *J Biol Chem* 2002;277(5):3195–201 Epub 2001/11/08.
- [16] Morgani SM, Saiz N, Garg V, Raina D, Simon CS, Kang M, et al. A Sprouty4 reporter to monitor FGF/ERK signaling activity in ESCs and mice. *Dev Biol* 2018;441(1):104–26 Epub 2018/07/03.
- [17] Lo TL, Yusoff P, Fong CW, Guo K, McCaw BJ, Phillips WA, et al. The ras/mitogen-activated protein kinase pathway inhibitor and likely tumor suppressor proteins, sprouty 1 and sprouty 2 are deregulated in breast cancer. *Cancer Res* 2004;64(17):6127–36 Epub 2004/09/03.
- [18] Fong CW, Chua MS, McKie AB, Ling SH, Mason V, Li R, et al. Sprouty 2, an inhibitor of mitogen-activated protein kinase signaling, is down-regulated in hepatocellular carcinoma. *Cancer Res* 2006;66(4):2048–58 Epub 2006/02/21.
- [19] Patel R, Gao M, Ahmad I, Fleming J, Singh LB, Rai TS, et al. Sprouty2, PTEN, and PP2A interact to regulate prostate cancer progression. *J Clin Investig* 2013;123(3):1157–75 Epub 2013/02/26.
- [20] Frolov A, Chahwan S, Ochs M, Arnoletti JP, Pan ZZ, Favorova O, et al. Response markers and the molecular mechanisms of action of gleevec in gastrointestinal stromal tumors. *Mol Cancer Ther* 2003;2(8):699–709 Epub 2003/08/27.
- [21] Feng YH, Tsao CJ, Wu CL, Chang JG, Lu PJ, Yeh KT, et al. Sprouty2 protein enhances the response to gefitinib through epidermal growth factor receptor in colon cancer cells. *Cancer Sci* 2010;101(9):2033–8 Epub 2010/07/14.
- [22] Faratian D, Sims AH, Mullen P, Kay C, Um I, Langdon SP, et al. Sprouty 2 is an independent prognostic factor in breast cancer and may be useful in stratifying patients for trastuzumab therapy. *PLoS ONE* 2011;6(8):e23772. Epub 2011/09/13.
- [23] Sirivatanauksorn Y, Sirivatanauksorn V, Srisawat C, Khongmanee A, Tongkham C. Differential expression of sprouty genes in hepatocellular carcinoma. *J Surg Oncol* 2012;105(3):273–6 Epub 2011/09/21.
- [24] Xu Y, Yang X, Li Z, Li S, Guo S, Ismail S, et al. Sprouty2 correlates with favorable prognosis of gastric adenocarcinoma via suppressing FGFR2-induced ERK phosphorylation and cancer progression. *Oncotarget* 2017;8(3):4888–900 Epub 2016/12/22.
- [25] Celik-Selvi BE, Stutz A, Mayer CE, Salhi J, Siegwart G, Sutterluty H. Sprouty3 and Sprouty4, two members of a family known to inhibit FGF-Mediated signaling, exert opposing roles on proliferation and migration of glioblastoma-derived cells. *Cells* 2019;8(8) Epub 2019/08/04.
- [26] Tennis MA, Van Scoyk MM, Freeman SV, Vandervest KM, Nemenoff RA, Winn RA. Sprouty-4 inhibits transformed cell growth, migration and invasion, and epithelial-mesenchymal transition, and is regulated by WNT17A through PPARgamma in non-small cell lung cancer. *Mol Cancer Res: MCR* 2010;8(6):833–43 Epub 2010/05/27.
- [27] Masoumi-Moghaddam S, Amini A, Wei AQ, Robertson G, Morris DL. Sprouty 2 protein, but not Sprouty4, is an independent prognostic biomarker for human epithelial ovarian cancer. *Int J Cancer* 2015;137(3):560–70 Epub 2015/01/30.
- [28] Zhao Z, Chen CC, Rillahhan CD, Shen R, Kitzing T, McNerney ME, et al. Cooperative loss of RAS feedback regulation drives myeloid leukemogenesis. *Nat Genet* 2015;47(5):539–43 Epub 2015/03/31.
- [29] Xu YF, Liu HD, Liu ZL, Pan C, Yang XQ, Ning SL, et al. Sprouty2 suppresses progression and correlates to favourable prognosis of intrahepatic cholangiocarcinoma via antagonizing FGFR2 signalling. *J Cell Mol Med* 2018;22(11):5596–606 Epub 2018/08/31.
- [30] Xu YF, Ge FJ, Han B, Yang XQ, Su H, Zhao AC, et al. High-mobility group box 1 expression and lymph node metastasis in intrahepatic cholangiocarcinoma. *World J Gastroenterol* 2015;21(11):3256–65 Epub 2015/03/26.
- [31] Azim Jr. HA, Peccatori FA, Brohee S, Branstetter D, Loi S, Viale G, et al. RANK-ligand (RANKL) expression in young breast cancer patients and during pregnancy. *Breast Cancer Res: BCR* 2015;17:24. Epub 2015/04/08.
- [32] Yeo W, Chan SL, Mo FK, Chu CM, Hui JW, Tong JH, et al. Phase I/II study of temsirolimus for patients with unresectable hepatocellular carcinoma (HCC)- a correlative study to explore potential biomarkers for response. *BMC Cancer* 2015;15:395. Epub 2015/05/13.
- [33] Liu H, Xu Y, Zhang Q, Yang H, Shi W, Liu Z, et al. Prognostic significance of TBL1XR1 in predicting liver metastasis for early stage colorectal cancer. *Surg Oncol* 2017;26(1):13–20 Epub 2017/03/21.
- [34] Wang HM, Xu YF, Ning SL, Yang DX, Li Y, Du YJ, et al. The catalytic region and pest domain of PTPN18 distinctly regulate the HER2 phosphorylation and ubiquitination barcodes. *Cell Res* 2014;24(9):1067–90 Epub 2014/08/02.
- [35] Xu YF, Yang XQ, Lu XF, Guo S, Liu Y, Iqbal M, et al. Fibroblast growth factor receptor 4 promotes progression and correlates to poor prognosis in cholangiocarcinoma. *Biochem Biophys Res Commun* 2014;446(1):54–60 Epub 2014/02/26.
- [36] Guy GR, Wong ES, Yusoff P, Chandramouli S, Lo TL, Lim J, et al. Sprouty: how does the branch manager work? *J Cell Sci* 2003;116(Pt 15):3061–8 Epub 2003/06/28.
- [37] Farges O, Fuks D, Le Treut YP, Azoulay D, Laurent A, Bachellier P, et al. AJCC 7th edition of TNM staging accurately discriminates outcomes of patients with resectable intrahepatic cholangiocarcinoma: by the AFC-IHCC-2009 study group. *Cancer* 2011;117(10):2170–7 Epub 2011/04/28.
- [38] Byron SA, Gartside MG, Wellens CL, Mallon MA, Keenan JB, Powell MA, et al. Inhibition of activated fibroblast growth factor receptor 2 in endometrial cancer cells induces cell death despite PTEN abrogation. *Cancer Res* 2008;68(17):6902–7 Epub 2008/09/02.
- [39] Rizvi S, Borad MJ. The rise of the FGFR inhibitor in advanced biliary cancer: the next cover of time magazine? *J Gastrointest Oncol* 2016;7(5):789–96 Epub 2016/10/18.
- [40] Goyal L, Saha SK, Liu LY, Siravegna G, Leshchiner I, Ahronian LG, et al. Polyclonal secondary FGFR2 mutations drive acquired resistance to FGFR inhibition in patients with FGFR2 fusion-positive cholangiocarcinoma. *Cancer Discov* 2017;7(3):252–63 Epub 2016/12/31.